



Calcination and Microwave Assisted Biological Synthesis of Iron Oxide Nanoparticles and Comparative Efficiency Studies for Domestic Wastewater Treatment

Herlekar Mihir and Barve Siddhivinayak

Department of Botany, KET's V.G. Vaze College of Arts, Science and Commerce, Mulund (E), Mumbai, INDIA

Available online at: www.isca.in, www.isca.me

Received 14th March 2015, revised 24th April 2015, accepted 2nd June 2015

Abstract

Owing to the limitations of conventional synthesis methods for iron nanoparticles and its wide range of environmental applications, there is a need to develop green synthesis protocols by exploring newer biological resources. In this study, for the first time, Turmeric (*Curcuma longa* L.) leaves were used to synthesize iron oxide nanoparticles by calcination ($Fe\ NP_{Cal}$) and microwave assisted method ($Fe\ NP_{Mw}$). The characterization of magnetic nanoparticles was done by different techniques. As prepared nanoparticles were compared for their efficiency to treat domestic wastewater in terms of orthophosphate (PO_4), Chemical Oxygen Demand (COD) and *Escherichia coli* (*E. coli*) removal. $Fe\ NP_{Mw}$ showed higher removal efficiency of PO_4 and COD (82% and 83% respectively) than $Fe\ NP_{Cal}$ (17%, 82% respectively) in 24 hours. $Fe\ NP_{Cal}$ exhibited superior antimicrobial activity than $Fe\ NP_{Mw}$ and completely inhibited *E. coli*.

Keywords: Iron oxide nanoparticles, green synthesis, *Curcuma Longa* L., calcination, microwave, domestic wastewater.

Introduction

Water is one of the most important and basic natural resources. Owing to increasing industrialization and exploding population, there is continuous increase in demand of water supply. On the other hand, the problem of water pollution is getting very severe, especially in developing countries with disposal of untreated sewage. This disposal has resulted in additional load of inorganic, organic and microbial pollutants which further deteriorates the water quality^{1,2}. Conventionally, the pollutants from sewage are removed to a certain extent in wastewater treatment facilities (WWTFs). But, the major limitations of existing WWTFs include time required for the complete process (around 15-20 hours), installation, maintenance, labor and energy cost along with the sludge handling. So, the researchers need to develop advanced technologies which are cost effective, durable and more efficient as compared to the existing treatment options. In this context, "Nanotechnology" could help in solving the problems concerning water purification and quality³.

Iron nanoparticles, namely nano zero-valent iron (nZVI), magnetite (Fe_3O_4) and maghemite ($\gamma\text{-}Fe_2O_3$) are widely used in the field of environmental remediation. This is mainly due to their very efficient pollutant removal capacity, fast reaction kinetics and most importantly due to magnetism which enables its easy recovery⁴. These nanoparticles, when synthesized by conventional physical and chemical methods, lose their reactivity due to aggregate formation⁵ and magnetism and dispersibility on air exposure⁶. In addition to these limitations, the concern arising due to use of non polar solvents and toxic reducing agents such as sodium borohydride during synthesis

have not only limited their environmental application but also have highlighted the need to develop clean, non toxic and environment friendly procedures for iron nanoparticle synthesis.

Plant-mediated synthesis of magnetic nanoparticles has remained a relatively unexplored research area with the majority of papers being published only in the last two years⁷. In the present study, for the first time, Turmeric (*Curcuma longa* L.) leaves were used as biotemplate for iron nanoparticle synthesis. India is the largest producer, consumer and exporter of Turmeric (*Curcuma longa* L.)⁸. The turmeric rhizomes are widely used but the leaves, except for its use in Indian and Malaysian cooking, are mostly treated as an agro-waste⁹. The magnetic nanoparticles were synthesized by two methods - calcination and microwave assisted synthesis. The iron nanoparticles synthesized by both these methods were characterized and tested for their efficiency to treat municipal wastewater. This is the first of its kind study that evaluates the efficiency of biologically synthesized magnetic nanoparticles for the treatment of municipal wastewater in terms of COD, *E. coli* and PO_4 removal.

Material and Methods

Turmeric (*Curcuma longa* L.) leaves were obtained from farm in Satara district in Maharashtra. The leaves were repeatedly washed with double distilled water and sun dried. These were further dried in an oven (Metalab) at 50^o C for 48 hours, fine powdered using domestic blender and stored in air tight container and used as biotemplate. From now on, it is denoted as turmeric leaf powder (TLP).

purified anhydrous iron (III) chloride (FeCl_3), pure sodium chloride (NaCl), concentrated sulfuric acid (H_2SO_4), silver sulfate (Ag_2SO_4), ammonium iron (II) sulfate hexahydrate [$(\text{NH}_4)_2\text{Fe}(\text{SO}_4)_2 \cdot 6\text{H}_2\text{O}$], ferroin indicator were purchased from erck India. Potassium dichromate ($\text{K}_2\text{Cr}_2\text{O}_7$), Mercuric sulfate (HgSO_4), Ammonium molybdate, stannous chloride and liquor ammonia solution was obtained from Qualigens Fine Chemicals Pvt. Ltd. India. All the chemicals were of analytical grade and were used without further purification. M-EC Test Agar was purchased from Hi Media, India.

Synthesis of Iron Oxide Nanoparticles: Calcination Method: 9 grams of FeCl_3 was dissolved in 150 ml saturated NaCl solution and 18 grams of TLP was added to it. This mixture was kept on a rotary shaker at 100 rpm overnight. The plant material was then separated by vacuum filtration and filter residue was washed with double distilled water to remove any unbound FeCl_3 . It was then dried overnight in an oven at 80°C . The dried material was calcined in a muffle furnace at 450°C for 6 hours. After cooling to room temperature in a desiccator, the calcined material was homogenized using mortar and pestle¹⁰.

Microwave Method: 8 grams of plant material was added to 1 M FeCl_3 solution and kept on a rotary shaker at 100 rpm for 9 hours. Excess FeCl_3 was decanted and the plant material was microwaved for 2 minutes at 15 seconds interval. The plant material was then immersed in 5 M liquor ammonia solution for 24 hours. Excess ammonia solution was then decanted and microwaved for 3 minutes at 1 minute interval. The alkali treated material was rinsed several times with double distilled water and finally microwaved for 4 minutes at 30 seconds interval¹¹. The dried material was homogenized using mortar and pestle.

Characterization of Iron Oxide Nanoparticles: The preliminary characterization of nanoparticles was done using Chemito UV-Visible spectrophotometer (Model UV 2100) after recovering the embedded nanoparticles from the plant matrix. For this purpose, the nanocomposites were sonicated for 5 minutes in double distilled water and then centrifuged at 1000 rpm for 5 minutes so that TLP gets separated. The procedure was repeated thrice to ensure maximum recovery. The morphological features and elemental composition of as-synthesized nanocomposites was analyzed using SEM-EDX (FEI ESEM Quanta 200). To identify the phase of iron oxide formed, X-Ray Diffraction (XRD) analysis was done using Shimadzu 6000 with $\text{Cu-K}\alpha$ radiation source with wavelength of 0.154 nm and was operated at 40kV/30mA over 2θ range of 2 to 80. The scanning speed was maintained at 50 min^{-1} . Fourier Transform Infrared Spectroscopy (FTIR) analysis of TLP and nanocomposite was done over the range of wave number 4000-400 cm^{-1} . The measurements were carried out on Perkin Elmer Spectrum BX FTIR spectrophotometer.

Domestic Wastewater Treatment Efficiency Comparison: The nanoparticles were evaluated for their efficiency to treat domestic sewage collected from a municipal wastewater

treatment facility located in Mumbai, India. pH was measured using pH meter. Initial and final concentration of COD, *E.coli* and PO_4 was measured by Open Reflux Method, Plate Count Method and Stannous Chloride Method respectively as per the Standard Methods for Water and Wastewater Analysis¹². A dose of 1 gramL^{-1} of nanoparticles was added to wastewater. The solution was stirred at 160 rpm at room temperature without any pH adjustment for 24 hours. After treatment, the nanocomposites were magnetically separated and the supernatant was filtered through Whatman® Grade GF/C filter paper and the filtrate was analyzed for PO_4 , COD and *E. coli*. All the experiments were done in triplicates and average values are reported.

Results and Discussion

Characteristics of raw sewage: The average initial concentration of PO_4 was 2.10, COD was 353 mg L^{-1} and *E. coli* count in raw sewage was $4.9 \times 10^7/100 \text{ ml}$ at pH 7.3.

Characterization of nanoparticles: The UV- vis spectra of supernatant solution containing nanoparticles was taken against the spectra of double distilled water as blank. The UV-visible spectra were scanned over the 300- 700 nm range. The formation of iron nanoparticles was confirmed by the characteristic peak at 423 nm in case of $\text{Fe NP}_{\text{Cal}}$ as depicted in figure-1a. Similar observation was noted in the study in which green synthesis of iron oxide nanoparticles was achieved by leaf extract of *Rumex acetosa* plant and the characteristic peak was observed at 420 nm^{13} . Fe NP_{MW} showed characteristic peak of magnetite at 377 nm as depicted in figure-1b¹⁴.

SEM images of $\text{Fe NP}_{\text{Cal}}$ are seen in figure-2a. As-synthesized nanoparticles were in cuboid and pyramid shaped. Similar observation was noted by when tea waste was used as template for magnetite synthesis¹⁰. The nanoparticles were found to be evenly dispersed in the plant matrix. Sodium chloride acted as spacer and thus prevented the formation of aggregated nanoparticles. Evenly dispersed spherical iron nanoparticles synthesized by microwave assisted protocol are shown in figure-2b¹¹.

The elemental composition of $\text{Fe NP}_{\text{Cal}}$ and Fe NP_{MW} studied using EDS is exhibited in figure-3a and figure-3b respectively. As can be seen from the figures, the predominant peaks were of iron (Fe), Oxygen (O) and Carbon (C). This confirmed the presence of Fe in the synthesized nanoparticles. The signals for C and O were mainly due to the different phytochemicals present in turmeric leaf powder used during the synthesis. The signal for oxygen also confirms the fact that iron oxide nanoparticles have been synthesized. The weight percent (wt %) of elements in $\text{Fe NP}_{\text{Cal}}$ was measured to be 41.72% for Fe, 35.03 % for O and 20.03 % for C. Some minor loading from sodium (Na) and (Cl) was also observed. It would be arising from the use of NaCl as spacer. 1.98 wt % of Na and 1.23 % of Cl was detected. The Fe content in Fe NP_{MW} (25.52%) was

comparatively lesser than Fe NP_{Cal}. Other elements observed were 36.98% of Carbon and 35.99% of Oxygen in addition to traces of Silica (Si) arising from plant material. The high Fe loading enables easy recovery of as-prepared nanoparticles.

XRD patterns obtained for Fe NP_{Cal} is shown in figure-4a. The diffraction peaks were observed at 2θ values of 31.730, 45.450 and 66.250. The peak at 31.730 can be indexed to the formation of magnetite. The peak at 45.450 corresponds to Fe with associated peak at 66.250 matching with the XRD standard for the magnetite nanoparticles¹⁵. Figure-4b shows XRD of Fe NP_{MW}. The diffraction peaks were observed at 2θ values of 29.67, 35.47 and 44.52. The peaks at 29.67 and 35.47 can be indexed to the formation of magnetite¹⁶. The peak at 44.52 corresponds to zero valent iron nanoparticles^{11,17}.

The crystallite size of iron nanoparticles was estimated using the Debye-Scherrer equation, which gives a relationship between peak broadening in XRD and particle size that is demonstrated by following equation:

$$d = k\lambda / (\beta \cdot \cos \theta) \tag{1}$$

where, d is the particle size of the crystal, k is Scherrer constant, λ is the X-ray wavelength (0.154 nm), β is the width of the XRD peak at half-height, and θ is the Bragg diffraction angle. Using the Scherrer equation the average crystallite sizes of the magnetic nanoparticles synthesized by calcination method was estimated to be in the range of 66 to 148 nm. Whereas, those synthesized by microwave method were smaller; in size range of 17.9 to 28.7 nm. The size of nZVI was calculated to be 23.8 nm.

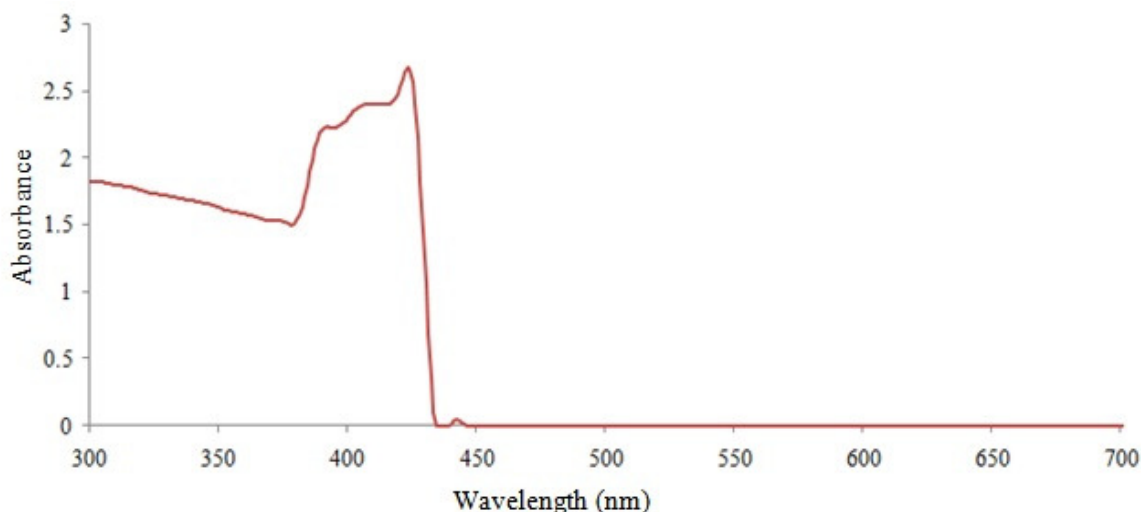


Figure-1a
 UV-visible Absorption Spectra of Fe NP_{Cal}

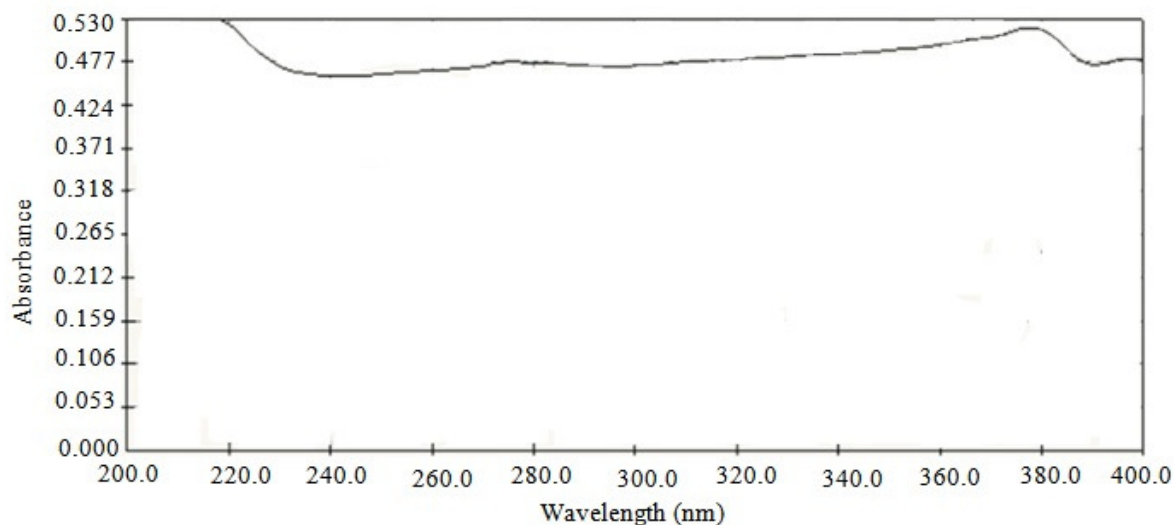


Figure-1b
 UV-visible Absorption Spectra of Fe NP_{MW}

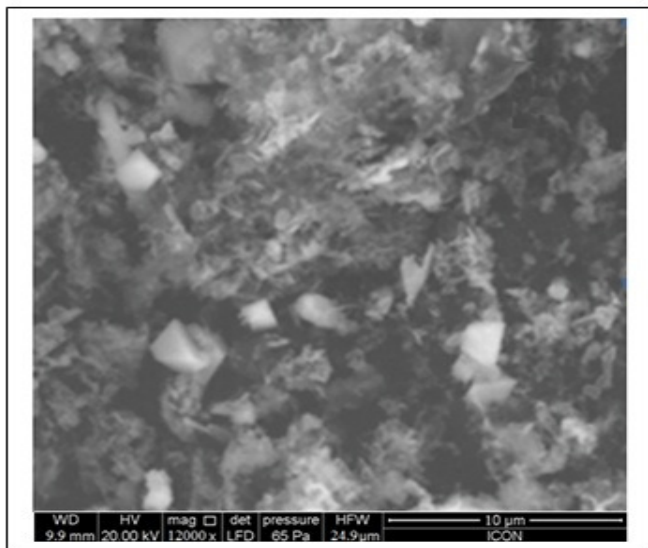


Figure-2a
SEM Image of Fe NP_{Cal}

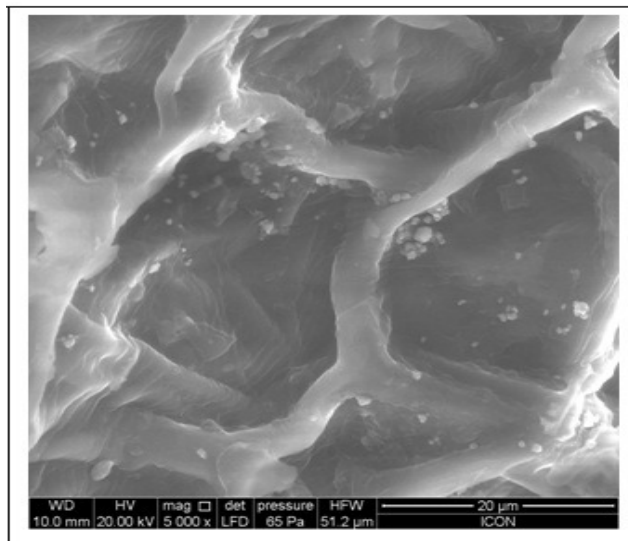


Figure-2b
SEM Image of Fe NP_{MW}

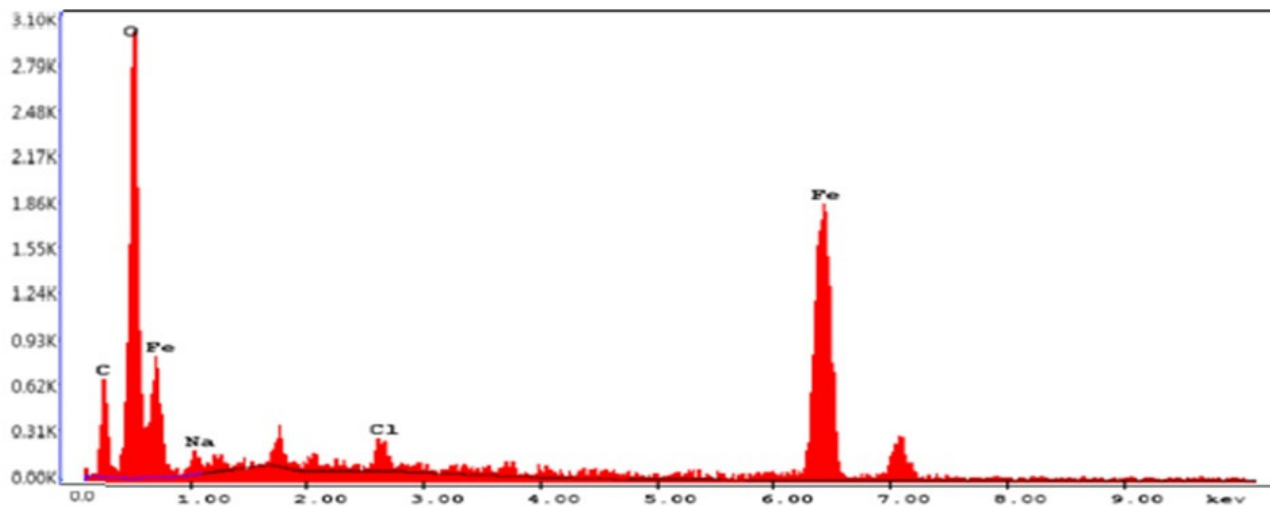


Figure-3a
Elemental Composition of Fe NP_{Cal}

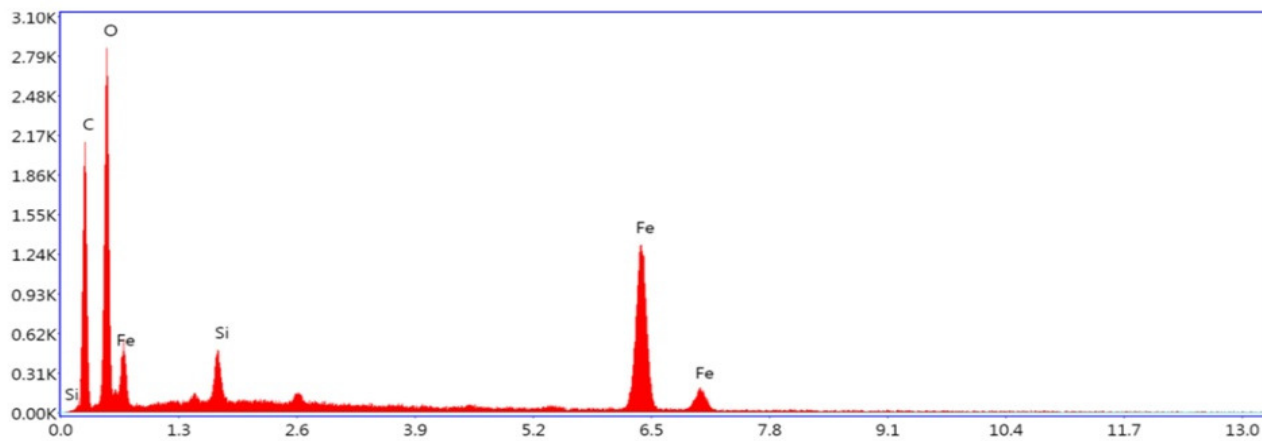


Figure-3b
Elemental Composition of Fe NP_{MW}

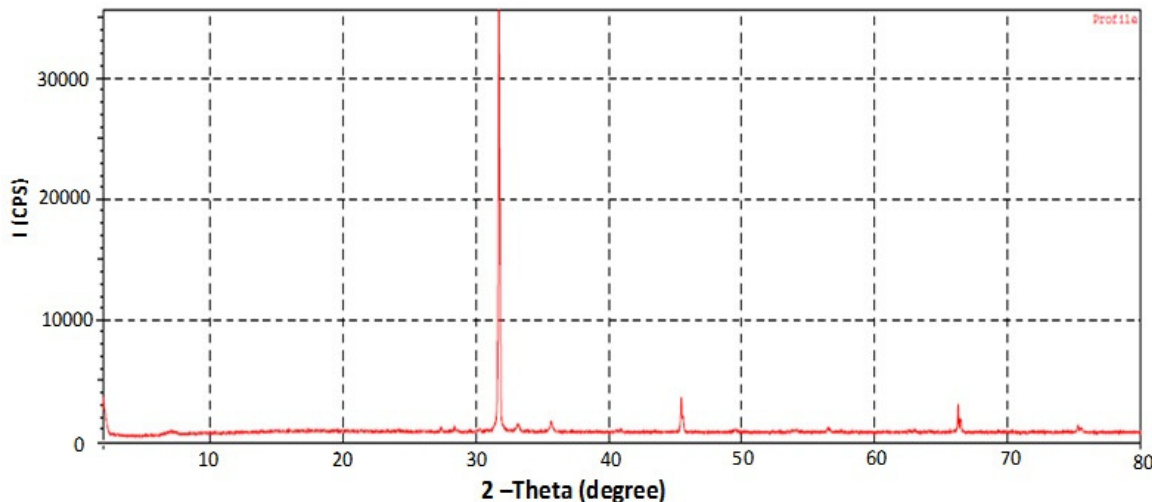


Figure-4a
XRD Pattern of NP_{Cal}

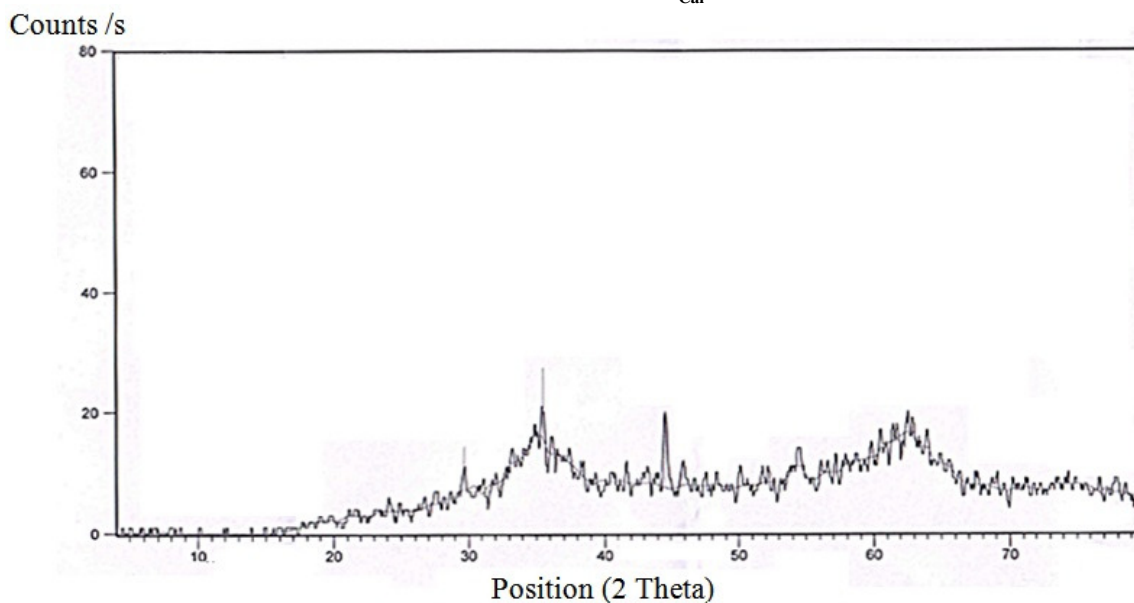


Figure-4b
XRD Pattern of NP_{MW}

Mechanism of Magnetite synthesis: FTIR measurements of TLP and nanoparticles (figure-5a, 5b and 5c) were carried out to understand the involvement of biomolecules in nanoparticle synthesis. Turmeric leaves have high polyphenol content^{9,18} and authors have already highlighted its role in forming complex with metal ions and reduce the metals^{19,20}.

The shift in the FTIR peaks of TLP from 3260.43 (attributed to O-H stretch) to 3289.30 in FTIR spectra of oven dried material indicated involvement of polyphenols from TLP in reduction of iron. Also, involvement of aldehydes group can be seen in peak shift from 1670.10 in TLP to 1643.37 in oven dried material. Oxidation of reduced Fe in oven dried material to iron oxide during calcination resulted in the formation of Fe NP_{Cal} and was confirmed by the peaks at 636.16 cm⁻¹ and 585.38 cm⁻¹ which

are attributed to Fe-O bond vibration of Fe₃O₄²¹.

Calcined material also shows strong and broad absorption band at 3367.44 cm⁻¹ due to stretching vibration of -OH which can be assigned to OH- absorbed by iron oxide nanoparticles. The peak at 2923.53 cm⁻¹ and 2338.47 cm⁻¹ can be attributed to C-H stretching of aliphatic carbon. These peaks along with peaks at 1090 cm⁻¹ (C-O stretch), 798.20 cm⁻¹ (C-H stretch) indicate that minute quantity of residual carbon of turmeric leaves is present in Fe NP_{Cal} even after calcination. The peak at 1634.11 cm⁻¹ indicates C=O stretch of aldehydes in turmeric leaves²².

In iron oxide nanoparticles synthesized by microwave method, involvement of polyphenols and aldehydes in turmeric leaves is highlighted by the shift of peak to 3420.37 cm⁻¹ and 1628.13 cm⁻¹ respectively in microwaved material. Alkali treatment and

further microwaving has resulted the formation of reduced iron nanoparticles¹¹. Iron oxide peaks are characterized by strong bands in low wavelength region of 1000-400 cm⁻¹. The peak at 827.61 cm⁻¹ is attributed to Fe-OH vibration²³.

Sewage Treatability Studies: The comparative percent removal of pollutants under study is depicted in figure-6. Plant material ash without iron nanoparticles resulted in slight increase in PO₄ concentration; this is commonly reported for biochars prepared from biomass²⁴. Low PO₄ removal by Fe NP_{Cal} can be attributed to ash content in the chosen plant materials (around 15 wt % of ash was generated when only turmeric leaves were calcined). The silicates being negatively charged results in the repulsion of negatively charged phosphate ions from the sewage sample²⁵. Other reasons attributed to low

PO₄ removal can be trapping of iron oxide in the residue of calcined biomass making it less available for adsorption which highlights the importance of adsorbent preparation temperature on the location of iron oxide in the composite²⁶. Eucalyptus leaves extract synthesized iron nanoparticles have been reported to remove 30.4% of total phosphorus from swine wastewater²⁷. Only plant material treated with alkali and microwave resulted in 32% of PO₄ removal. In case of Fe NP_{MW}, significantly higher PO₄ removal was observed. The reason for high efficiency of this nanocomposite in PO₄ removal is due to its ability to form monodentate inner sphere complex with phosphorus at around neutral pH which holds true for sewage²⁸. Highly efficient phosphorus adsorbing magnetic nanocomposites have been previously synthesized for phosphate removal from synthetic samples¹¹.

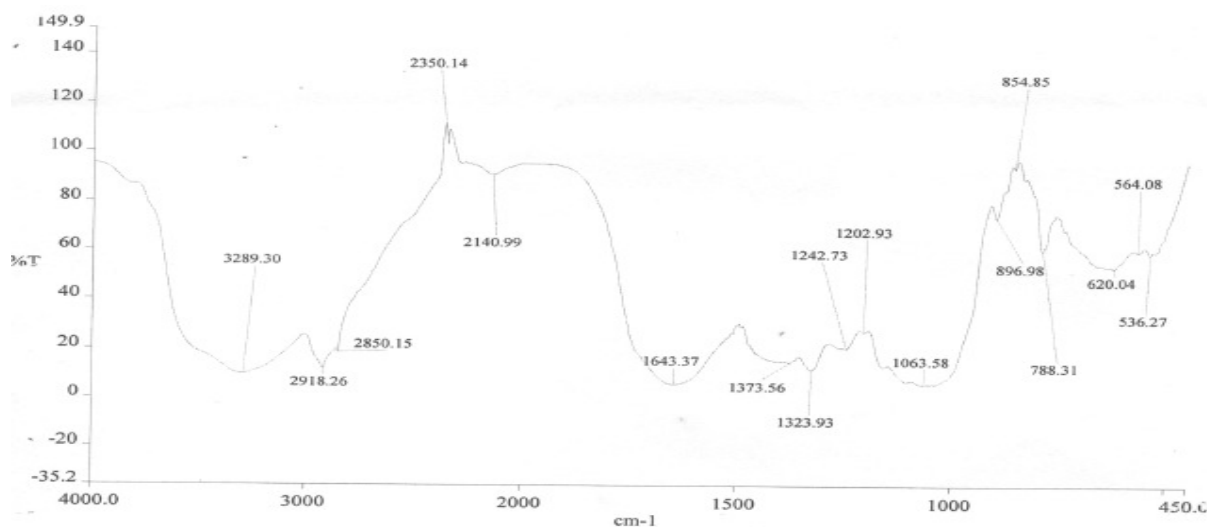


Figure-5a
 FTIR Measurements of TLP

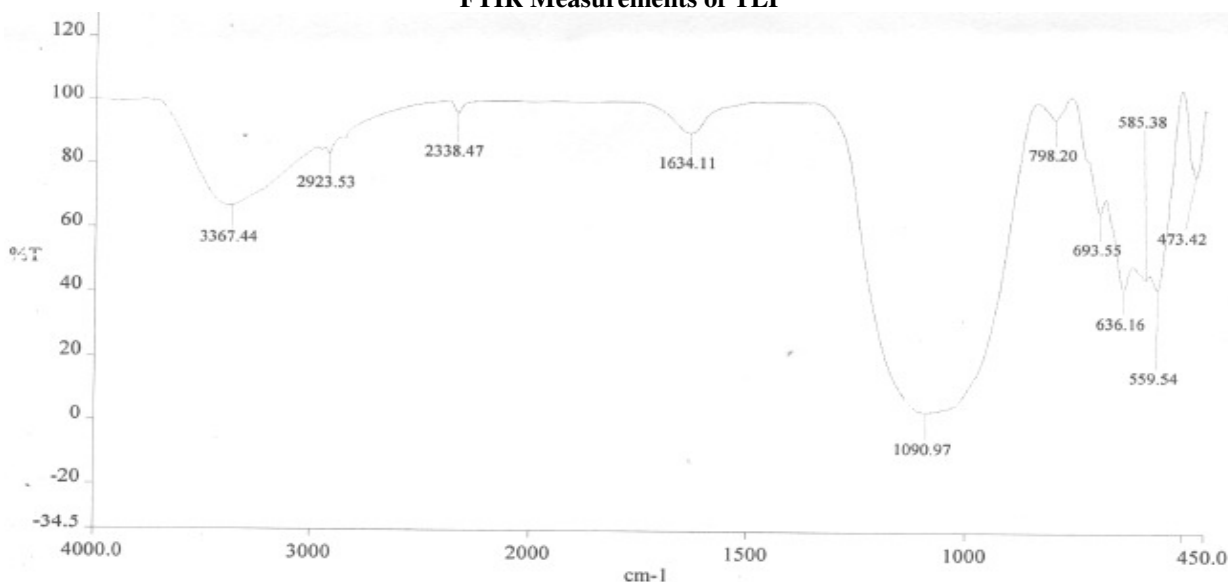


Figure-5b
 FTIR Measurements of NP_{Cal}

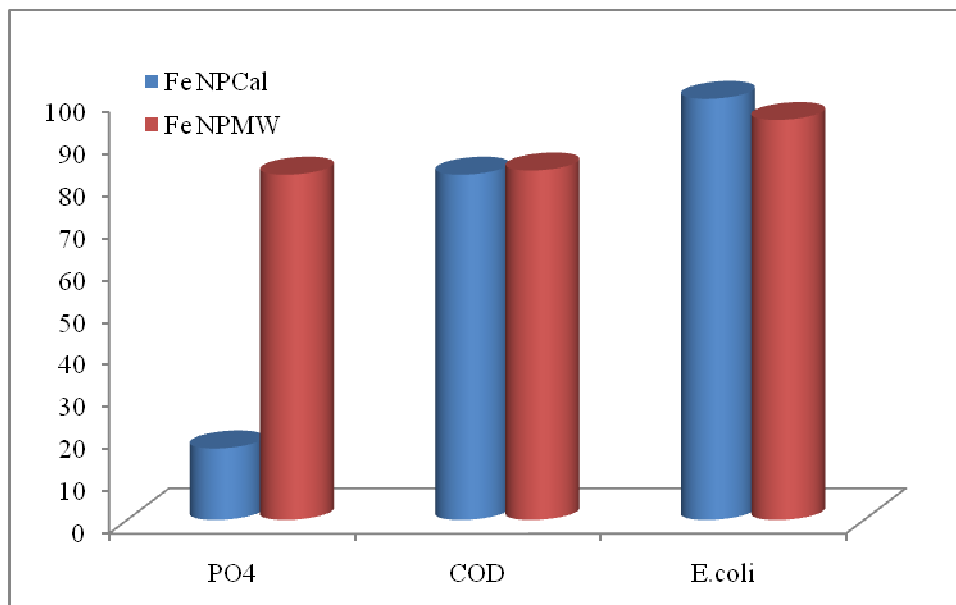


Figure-6
Comparison of Percent Pollutant Removal

Calcined plant material resulted in 78% COD reduction. The iron nanocomposite by calcinations method could remove 82% COD from the domestic wastewater within 24 hours. The calcination at low temperature has been reported to result in the formation of porous structure due to the elimination of biotemplate which resulted in adsorption of organic matter²⁶. Higher ash content also might have led to better COD removal²⁹. Only 44% reduction was achieved using plant material treated with alkali and subsequent microwaving. Fe NP_{MW} removed 83% of COD from domestic sewage sample. The amount of iron/iron oxide incorporated into in the composite played an important role in organic matter removal¹¹. Not much literature could be cited with regards to COD removal from actual wastewater. However, one of the studies reported the efficacy of 84.5% of COD removal in 21 days from swine wastewater²⁰. Similarly, chemically synthesized 5% modified neodymium-doped TiO₂ nanoparticles could remove 95% of COD from municipal wastewater in 3 hours in presence of sunlight³⁰.

The growth of *E. coli* was completely inhibited using plant material ash as well as synthesized Fe NP_{Cal}. Reactive Oxygen Species (ROS) are known to cause damage to proteins and DNA in bacteria^{31,32}. The same mechanism seems to exhibit antimicrobial activity in the present study. The other reason could be trapping of microbial cells by amine groups in the nanocomposite as indicated by peaks at 1304.09 cm⁻¹ in FTIR of the microwaved nanocomposite. *E. coli* cells were successfully trapped by amino acid functionalized magnetic nanoparticles³³. The efficiency of percent removal of *E. coli* by microwaved plant material and Fe NP_{MW} seems to be comparable with that nanocomposite obtained by calcination method. But, the count is too high than the discharge standard of 10,000 CFU /100 ml

for the discharge of treated sewage as per India's Central Pollution Control Board norms³⁴. Effective inhibition of *E. coli* has been reported for nZVI synthesized by *Dodonaea viscosa* leaf extract³⁵.

Further studies are being carried out to understand the reaction kinetics and adsorption mechanism for removal of pollutants.

Conclusion

In this study, for the first time, magnetite nanoparticles were successfully synthesized using low-cost, renewable, eco-friendly biotemplate like turmeric leaves. The nanoparticles synthesized by calcination and microwave method were characterized using different techniques. Another innovative feature of this study is the comparative efficiency estimation of the as prepared nanocomposites for the municipal wastewater treatment at room temperature and without any pH adjustment. Fe NP_{Cal} exhibited significant COD removal capacity and excellent antimicrobial activity whereas, significantly higher PO₄ removal and almost similar COD removal was achieved using nanocomposites synthesized by microwave method. This underlines future potential of both these nanoadsorbents for the treatment of municipal wastewater and other industrial effluents.

Acknowledgement

Authors gratefully acknowledge the technical support from the KET's V. G. Vaze College and CSIR-NEERI, Mumbai Zonal Laboratory.

References

1. Koul N., Lokhande R.S. and Dhar J.K., Physico-

- Chemical, Bacteriological and Pesticide analysis of Tap Water in Millennium City Gurgoan, Haryana, India, *I. Res. J. Environment Sci.*, **1(2)**, 1-7 (2012)
2. Jesu A., Prabudoss Kumar L., Kandasamy K. and Dheenadayalan M.S., Environmental Impact of Industrial Effluent in Vaigai River and the Ground Water in and around the River at Anaipatti of Dindigul Distt, Tamil Nadu, India, *I. Res. J. Environment Sci.*, **2(4)**, 34-38 (2013)
 3. Tiwari A., and Kathane P., Superparamagnetic PVA-Alginate Microspheres as Adsorbent for Cu²⁺ ions Removal from Aqueous Systems, *I. Res. J. Environment Sci.*, **2(7)**, 44-53 (2013)
 4. Tang S.C. and Lo I. M., Magnetic Nanoparticles : Essential Factors for Sustainable Environmental Applications, *Water Res.*, **47(8)**, 2613-2632 (2013)
 5. Kim J. H., Tratnyek P. G. and Chang Y. S., Rapid Dechlorination of Polychlorinated Dibenzo-p-dioxins by Bimetallic and Nanosized Zerovalent Iron, *Environ. Sci. Technol.*, **42(11)**, 4106-4112 (2008)
 6. Wu W., He Q. and Jiang C., Magnetic Iron Oxide Nanoparticles: Synthesis and Surface Functionalization Strategies, *Nanoscale Res. Lett.*, **3(11)**, 397-415 (2008)
 7. Herlekar M., Barve S. and Kumar R., Plant-Mediated Green Synthesis of Iron Nanoparticles *J. Nanoparticles*, Article ID **140614**, 9 (2014)
 8. Ravindran P. Chapter 1: Turmeric- The Golden Spice of Life, In *Turmeric: The Genus Curcuma. Medicinal and Aromatic Plants - Industrial Profiles*; Ravindran, P.; Nirmal Babu, K.; Sivaraman, K. (Eds.); *CRC Press: London*, 1-2 (2007)
 9. Arutselvi R., Balasaravanan T., Ponmurugan P., Muthu Saranji, N. and Suresh P., Phytochemical Screening and Comparative Study of Anti Microbial Activity of Leaves and Rhizomes of Turmeric Varieties, *Asian J. Plant Sci. Res.*, **2(2)**, 212-219 (2012)
 10. Lunge S., Singh S., Sinha A. J., Magnetic Iron Oxide (Fe₃O₄) Nanoparticles from Tea Waste for Arsenic Removal, *J. Magn. Magn. Mater.*, **356**, 21-31 (2014)
 11. Ramasahayam S., Gunawan G., Finlay C. and Viswanathan T., Renewable Resource-Based Magnetic Nanocomposites for Removal and Recovery of Phosphorous from Contaminated Waters, *Water Air Soil Poll.*, **223(8)**, 4853-4863 (2012)
 12. Eaton A. and Franson M., (Eds.) Standard Methods for the Examination of Water and Wastewater, *American Public Health Association: USA*, (2005)
 13. Makarov V., Makarova S., Love A., Sinitsyna O., Dudnik A., Yaminsky I., Taliansky M. and Kalinina N., Biosynthesis of Stable Iron Oxide Nanoparticles in Aqueous Extracts of *Hordeum vulgare* and *Rumex acetosa* Plants, *Langmuir*, **30 (20)**, 5982-5988 (2014)
 14. Behera S.S., Patra J.K., Pramanik K., Panda N., Thatoi H., Characterization and Evaluation of Antibacterial Activities of Chemically Synthesized Iron Oxide Nanoparticles, *World J. Nano Sci. Eng.*, **2(4)**, 196-200 (2012)
 15. Viswanathan T., Renewable Resource-based Metal Oxide-containing Materials and Applications of the Same. U.S. Patent 0233802 A1 (2013)
 16. Huang L., Weng X., Chen Z., Megharaj M. and Naidu R., Synthesis of Iron-based Nanoparticles using Oolong Tea Extract for the Degradation of Malachite Green, *Spectrochimica Acta Part A: Molecular and Biomolecular Spectroscopy*, **117**, 801-804 (2014)
 17. Kuang Y., Wang Q., Chen Z., Megharaj M. and Naidu R., Heterogeneous Fenton-like Oxidation of Monochlorobenzene using Green Synthesis of Iron Nanoparticles, *J. Colloid Interface Sci.*, **410**, 67-73 (2013)
 18. Yan S.W. and Asmah R., Comparison of Total Phenolic Contents and Antioxidant Activities of Turmeric Leaf, Pandan Leaf and Torch Ginger Flower, *J. Int. Food Res.*, **17**, 417-423 (2010)
 19. Tandon P., Shukla R. and Singh S., Removal of Arsenic (III) from Water with Clay-Supported Zerovalent Iron Nanoparticles Synthesized with the Help of Tea Liquor, *Ind. Eng. Chem. Res.*, **52(30)**, 10052-10058 (2013)
 20. Wang T., Jin X., Chen Z., Megharaj M. and Naidu R., Green Synthesis of Fe Nanoparticles using Eucalyptus Leaf Extracts for Treatment of Eutrophic Wastewater, *Sci. Total Environ.*, **466-467**, 210-213 (2014)
 21. Dhoble R. M., Lunge S., Bhole A.G. and Rayalu S., Magnetic Binary Oxide Particles (MBOP): A Promising Adsorbent for Removal of As (III) in Water, *Water Res.*, **45**, 4769-4781 (2012)
 22. Konwar M. and Baruah G.D., On the Nature of Vibrational Bands in the FTIR Spectra of Medicinal Plant Leaves, *Arch. Appl. Sci. Res.*, **3(1)**, 214-221 (2011)
 23. Sangeetha N. and Kumaraguru A.K., Antitumor Effects and Characterization of Biosynthesized Iron Oxide Nanoparticles Using Seaweeds of Gulf of Mannar, *Int. J. Pharm. Pharma. Sci.*, **7(2)**, 469-476 (2015)
 24. Yao Y., Gao B., Inyang M., Zimmerman A.R., Cao X., Pullammanappallil P. and Yang L., Biochar Derived from Anaerobically Digested Sugar Beet Tailings Biochar Derived from Anaerobically Digested Sugar Beet Tailings, *Biores. Technol.*, **102**, 6273-6278 (2011)
 25. Abbassi R., Yadav A., Kumar N., Huang S., Jaffe P., Modeling and Optimization of Dye Removal using "Green" Clay Supported Iron Nano-particles, *Ecol. Eng.*, **61(A)**, 366-370 (2013)

26. Zhao L., Yang H., Li S., Yu L., Cui Y., Zhao X and Feng S., The Effect of Aging Time and Calcination Temperature on the Magnetic Properties of α -Fe/Fe₃O₄ Composite, *J. Magn. Magn. Mater.*, **301**, 287-291 (2006)
27. Wang T., Jin X., Chen Z., Megharaj M. and Naidu R., Green Synthesis of Fe Nanoparticles using Eucalyptus Leaf Extracts for Treatment of Eutrophic Wastewater, *Sci. Total Environ.*, **466-467**, 210-213 (2014)
28. Sarkar S., Blaney L.M., Gupta A., Ghosh D. and Sengupta A.K., Arsenic Removal from Groundwater and Its Safe Containment in a Rural Environment: Validation of a Sustainable Approach, *Environ.Sci.Technol.*, **42**, 4268-4273 (2008)
29. Ghorbani M. and Eisazadeh H., Removal of COD, Color, Anions and Heavy Metals from Cotton Textile Wastewater by Using Polyaniline and Polypyrrole Nanocomposites Coated on Rice Husk Ash, *Composites B*, **45**, 1-7 (2013)
30. Shahmoradi B., Ibrahim I.A., Sakamoto N., Ananda S., Somashekar R., Row T.N. and Byrappa K., Photocatalytic Treatment of Municipal Wastewater Using Modified Neodymium Doped TiO₂ Hybrid Nanoparticles, *J. Environ. Sci. Health A Tox. Hazard Subst. Environ. Eng.*, **45**, 1248-1255 (2010)
31. Sies H., Physiological Society Symposium: Impaired Endothelial and Smooth Muscle Cell Function in Oxidative Stress: Oxidants and Antioxidants, *Exp. Physiol.*, **82**, 291-295 (1997)
32. Arokiyaraj S., Saravanan M., Udaya Prakash N.K., Valan Arasu M., Vijayakumar B. and Vincent S., Enhanced Antibacterial Activity of Iron Oxide Magnetic Nanoparticles Treated with *Argemone Mexicana L.* Leaf Extract: An In Vitro Study, *Mater. Res. Bull.*, **48**, 3323-3327 (2013)
33. Jin Y., Liu F., Shan C., Tong M. and Hou Y., Efficient Bacterial Capture with Amino Acid Modified Magnetic Nanoparticles, *Water Res.*, **50**, 124-134 (2014)
34. Central Pollution Control Board, Performance of Sewage Treatment Plants- Coliform Reduction. *Control of Urban Pollution Series : CUPS/ 69* (2008)
35. Kiruba Daniel S.C.G., Vinothini G., Subramanian N., Nehru K. and Sivakumar M., Biosynthesis of Cu, ZVI, and Ag Nanoparticles using *Dodonaea viscosa* Extract for Antibacterial Activity Against Human Pathogens, *J. Nanopart. Res.*, **15**, 1319 (2013)